Growth mechanism of tubular ZnO formed in aqueous solution

Wei, A.; Xu, C. X.; Yang, Y.; Huang, W.; Sun, Xiaowei; Dong, Zhili; Tan, Swee Tiam

2006

Wei, A., Sun, X., Xu, C. X., Dong, Z. L., Yang, Y., Tan, S. T., et al. (2006). Growth mechanism of tubular ZnO formed in aqueous solution. Nanotechnology, 17(6), 1740-1744.

https://hdl.handle.net/10356/95560

https://doi.org/10.1088/0957-4484/17/6/033

Growth mechanism of tubular ZnO formed in aqueous solution

A Wei[1,2], X W Sun[1,5], C X Xu[3], Z L Dong[4], Y Yang[1], S T Tan[1] and W Huang[2]

[1] School of Electrical and Electronic Engineering, Nanyang Technological University, Nanyang Avenue, 639798, Singapore
[2] Institute of Advanced Materials, Fudan University, Shanghai 200433, People's Republic of China
[3] Advanced Photonics Center, Department of Electronic Engineering, Southeast Univeristy, Nanjing 210096, People's Republic of China
[4] School of Materials Science and Engineering, Nanyang Technological University, Nanyang Avenue, 639798, Singapore
[5] Author to whom any correspondence should be addressed. E-mail: exwsun@ntu.edu.sg

Abstract

Tubular ZnO microstructural arrays were fabricated by a hydrothermal decomposition method. The dependence of the morphologies on the growth time and temperature was investigated in detail. An experiment was carried out to determine the mechanism of tubular ZnO formation. Our results showed that ZnO microtubes originated from an ageing process from ZnO microrods at a lower temperature (compared to the temperature when hydrothermal deposition of ZnO microrods was dominant) due to the preferential chemical dissolution of the metastable Zn-rich (0001) polar surfaces. A growth model was proposed based on the coexistence of hydrothermal deposition and dissolution of ZnO in the fabrication process.

1. Introduction

Zinc oxide (ZnO), with a direct band gap of 3.37 eV and a large exciton binding energy of 60 meV, is a multifunctional semiconductor material and has been widely investigated for its catalytic, electrical, optoelectronic and photochemical properties [1, 2]. Recently, nanostructured ZnO has generated great interest worldwide. The tubular structure of ZnO becomes particularly important because high porosity and large surface area are required to fulfil the demand for high efficiency and activity in numerous applications. For example, the development of new functional materials with high porosity is required for better and optimized performance of dye-sensitized photovoltaic cells, dimensionally stable anodes, metal–ion batteries, electrochemical supercapacitors, hydrogen storage and

release devices, biosensors, and gas sensors [1, 3]. To date, tubular ZnO has been synthesized by several research groups using various methods [1, 4–16].

The hydrothermal decomposition method provides a low cost solution to fabricate ZnO microtube/nanotube arrays because of the low temperature, high yield, scalable process and large area uniform micro/nanostructures [4, 17–20]. Besides using essential reactants of zinc salt, alkali or ammonia, some surfactants or molecular templates, such as ethylenediamine [18, 19], and cetyltrimethylammonium bromide [20], were often introduced into the reaction solution in order to favour nucleation and nanostructure growth in the general hydrothermal reaction.

However, the growth mechanism of ZnO microtube/nanotube in solution remains unclear. Vayssieres *et al* have obtained well-aligned ZnO microtubes in an ageing process at 90°C for two days, and assumed an etching effect to explain the formation of the tubular structure [1]. A similar mechanism was also adopted to explain the growth of hollow ZnO nanostructures [13]. Wang *et al* reported a different mechanism in forming tubular ZnO [4]. In their opinion, the nanowires formed first on the substrate and self-adjusted in a hexagonal circle before growing into tubes. According to Zhang *et al*, the reaction product NH_3 was thought to play an important role in the formation of the tubular structure in the hydrothermal process [8].

In this paper, we report a simple hydrothermal decomposition method to fabricate ZnO microtube arrays at a lower temperature in a shorter time (about 5 h). An experiment was carried out to investigate the growth mechanism of ZnO microtubes.

2. Experimental details

The reaction solution was prepared by adding the appropriate quantity of ammonia (25%) into 280 ml zinc chloride solution ($ZnCl_2$, 0.1 M) to adjust the pH value to 10.0, and then the as-prepared solution was poured equally into seven bottles with autoclavable screw caps. Copper strips, cleaned with acetone and deionized (DI) water in an ultrasonic cleaner, were vertically immersed into the reaction solution.

The bottles (with samples (a)–(f)) were heated at a constant temperature of 95 °C in an ordinary laboratory oven. Samples (a), (b) and (c) were taken out of the oven one by one after 20, 50 and 90 min, respectively. Then the oven was turned off and cooled down naturally. It took about 1.5 h to cool the oven down to room temperature (RT). Samples (d), (e) and (f) were taken out of the oven after that oven had been turned off for 1.5, 5 and 6 h. Sample (g) was grown at 95°C for 7 h. All of the as-grown samples were thoroughly washed with DI water and dried in air for further characterization.

The morphologies of the samples were examined by a JEOL scanning electron microscope (SEM). The crystal structures of the samples were characterized by x-ray

diffraction (XRD) using Cu Kα radiation under an accelerating voltage of 40 kV. A JEOL 2010 transmission electron microscope (TEM) operated at 200 kV was used to observe the high resolution TEM (HRTEM) images and the selected area electron diffraction (SAED) pattern.

3. Results and discussion

The SEM images of samples (a)–(f) formed under different growth processes are shown in figures 1(a)–(f). Sample (a) shows a rod-like morphology after growth at 95°C for 20 min (figure 1(a)). After 50 min, sample (b) becomes slightly taller and thicker, meanwhile, a regular hexagonal shape becomes more apparent, as shown in figure 1(b). After 90 min, the rod ends become flat, as shown in figure 1(c). However, the morphology of the rods changes after the heating is stopped and the temperature of oven dropped naturally from 95℃ to RT in 1.5 h, the corresponding sample (d) clearly shows small craterlets on top of the rods (figure 1(d)). As the time increases, the craterlets become bigger and bigger, and change into hollow cavities of ZnO tubes. Figures 1(e) and (f) are the images taken from sample (e) and sample (f) after cooling down for 5 and 6 h, respectively. These two images clearly show the same tubular structure. Due to the longer reaction time, sample (f), with a diameter of about 500 nm, wall thickness of 50 nm, and length of 3 μm, shows thinner walls than sample (e).

Growth at 95°C for a longer time does not change the morphology into a tubular structure in our experiment. As shown in figure 2(a), the morphology of sample (g) still remains rod-like with hexagonal a cross-section after growth at 95°C for 7 h. To show the uniform morphology in a large area, figure 2(a) was obtained with a low magnification. For comparison, having undergone the same reaction time (7 h), sample (f) shows a tubular structure, as shown in figures 2(b) and 1(f) with low and medium magnifications.

The XRD measurement shows a similar diffraction pattern for all of the samples. A representative XRD spectrum is shown in figure 3. As indexed in the pattern, all of the diffraction peaks match the wurtzite ZnO structure, with lattice constants of a = 3.250 Å and c = 5.207 Å. The lattice structures of the ZnO microtubes were imaged by HRTEM and SAED. Figure 4 shows a representative TEM image of the ZnO microtubes and its corresponding SAED pattern (upper-left inset). The obvious contrast of the insetted TEM image at the upper-right corner in figure 4 clearly shows the tube structure of the sample. The lattice fringes in the HRTEM with d-spacing of 0.52 nm match the interspacing of the (0001) planes of the wurtzite ZnO. These results demonstrate that the ZnO microstructures grew along the [0001] direction. Consistent with the XRD pattern, the clear lattice image and SAED pattern indicate good crystalline quality of the hydrothermally grown ZnO microstructures. No dislocations or stacking faults were observed in the area examined.

The following chemical reactions take place in the aqueous solution, resulting in the formation and dissolution of ZnO [4, 21],

$$\begin{aligned} &Zn^{2+} + NH_3 \bullet H_2O \longleftrightarrow Zn(NH_3)_4^{2+} \\ &\quad + OH^- \underset{\Delta}{\longleftrightarrow} ZnO + NH_3 + H_2O. \end{aligned} \tag{1}$$

In this reaction, the precursor $Zn(NH_3)_4^{2+}$ reacts with OH^- to form ZnO (the equilibrium in the above equation moves to the right), which is deposited on the substrate. This deposition reaction only happens at higher temperatures (>75 °C) [4]. The equilibrium move to the left leads to dissolution of ZnO.

The growth process of tubular ZnO could be divided into two stages (figure 5). The first stage corresponds to the transformation of a large amount of the precursor $Zn(NH_3)_4^{2+}$ into ZnO deposition through hydrothermal decomposition at a higher temperature of 95 °C (figures 5(a)–(c)). At the same time, ZnO also dissolves according to the reaction (1) as the equilibrium moves to the left. However, the growth of ZnO is dominant because the high concentration of $Zn(NH_3)_4^{2+}$ favours precipitation of ZnO at 95°C. The tower-like morphologies are due to the faster growth rate along the [0001] direction than those along other directions [22]. With the reaction going on, the concentration of $Zn(NH_3)_4^{2+}$ reduces, and the dissolution effect becomes more dominant, therefore, the ends of the rods become flat as shown in figures 1(c) and 5(c).

The second stage is called the ageing process, which corresponds to the dissolution of ZnO at lower temperature (<75°C). In this case, the dissolution effect is dominant because the hydrothermal decomposition is almost ceased at lower temperatures. The rate of ZnO dissolution is faster than that of deposition, so the preferential chemical dissolution of the top *(*0001*)* surfaces of the as-grown rods leads to the hollow structure shown in figures 1(d)–(f) and 5(d)–(e).

To explain why this ageing process results in the formation of tubular rods rather than thinning the rods, we look at the lattice structure of wurtzite ZnO. The ionic and polar structure of ZnO can be described as hexagonal close packing of oxygen and zinc atoms as shown in figure 6. They exhibit several crystal planes: a basal polar oxygen plane *(*$000\bar{1}$*)*, a top tetrahedron corner-exposed polar zinc (0001) face, and six low-index nonpolar $\{\bar{1}010\}$ planes parallel to the *c* axis. The nonpolar planes are the most stable ones, and the polar ones are metastable [1]. The dissolution rate of the polar plane (0001) is faster than that of the nonpolar plane $\{\bar{1}010\}$, so the (0001) atomic plane should be removed by dissolution faster than the $\{\bar{1}010\}$ plane. In figure 1(d), the sample (d) shows small craterlets on the top of rod due to dissolution. As the reaction continues, the wall

thickness of the tubular ZnO becomes thinner. In this paper, our reaction time (7 h) is not long enough to observe the shortening effect. For a longer reaction time (several days), the tubular structure could be shortened and even disappear. Therefore, the ageing process removes the atoms in the metastable (0001) planes, leading to the formation of tubular ZnO structures.

In our experiments, the complex ions of $Zn(NH_3)_4^{2+}$ would be partially consumed after around 90 min reaction time. The deposition rate of ZnO is almost equal to the dissolution rate at higher temperature, so only ZnO rods shown in figure 2(a) were observed in the growth process for 7 h heating at 95°C. However, a few craterlets appear on the top of some rods. So, in the case of very long heating times, the etching effect will be dominant after the complex ions of $Zn(NH_3)_4^{2+}$ are depleted so much that the balance between deposition and dissolution is disturbed. That is probably the reason why rod-like ZnO changed into tube-like ZnO at 90°C for 2 days, as reported by Vayssieres *et al* [1].

4. Conclusion

We performed an experiment to clearly elucidate the evolution of tubular ZnO in aqueous solution by a simple hydrothermal method carried out using a mixture of ammonia and $ZnCl_2$ solution at lower temperature. A two-stage growth model is proposed based on the coexistence of hydrothermal deposition and dissolution of ZnO in the fabrication process. The first growth stage corresponds to the precipitation of ZnO from $Zn(NH_3)_4^{2+}$ at a higher temperature. The second stage is an etching process, which happens when the precursor $Zn(NH_3)_4^{2+}$ is depleted at a high temperature or hydrothermal decomposition is ceased at a low temperature. The deposition and dissolution process can potentially be controlled to obtain uniform ZnO microrods and microtubes by adjusting the reaction time and temperature.

Acknowledgments

Sponsorship from the Research Grant Manpower Fund (RGM 21/04) of Nanyang Technological University, and a Science and Engineering Research Council Grant (No. 0421010010) from the Agency for Science, Technology and Research (A*STAR), Singapore are gratefully acknowledged.

References

[1] Vayssieres L, Keis K, Hagfeldt A and Lindquist S E 2001 *Chem. Mater.* **13** 4395

[2] Huang M H, Mao S, Feick H, Yan H Q, Wu Y Y, Kind H, Weber E, Russo R and Yang P D 2001 *Science* **292** 1897

[3] Yao Z, Postma H W Ch, Balents L and Dekker C 1999 *Nature* **402** 273

[4] Wang Z, Qian X F, Yin J and Zhu Z K 2004 *Langmuir* **20** 3441

[5] Hua J Q and Bando Y 2003 *Appl. Phys. Lett.* **82** 1401

[6] Abduev A Kh, Akhmedov A K, Baryshnikov V G and Shakhshaev Sh O 2000 *Tech. Phys. Lett.* **26** 332

[7] Wu J J, Liu S C, Wu C T, Chen K H and Chen L C 2002 *Appl. Phys. Lett.* **81** 1312

[8] Zhang J, Sun L D, Liao C S and Yan C H 2002 *Chem. Commun.* 262

[9] Sun X W, Yu S F, Xu C X, Yuen C, Chen B J and Li S 2003 *Japan. J. Appl. Phys.* **42** L1229 doi:10.1143/JJAP.42.L1229

[10] Hu J Q, Bando Y and Liu Z W 2003 *Adv. Mater.* **12** 1000

[11] Zhang X H, Xie S Y, Jiang Z Y, Zhang X, Tian Z Q, Xie Z X, Huang R B and Zheng L S 2003 *J. Phys. Chem.* B **107** 10114

[12] Wang R M, Xing Y J, Xu J and Yu D P 2003 *New J. Phys.* **5** 115.1

[13] Yu H D, Zhang Z P, Han M Y, Hao X T and Zhu F R 2005 *J. Am. Chem. Soc.* **127** 2378

[14] Zhang B P, Binh N T, Wakatsuki K, Segawa Y, Yamada Y, Usami N, Kawasaki M and Koinuma H 2004 *Appl. Phys. Lett.* **84** 4098

[15] Kong X H, Sun X M, Li X L and Li Y D 2003 *Mater. Chem. Phys.* **82** 997

[16] Jeong J S, Lee J Y, Cho J H, Suh H J and Lee C J 2005 *Chem. Mater.* **17** 2752

[17] Vayssieres L, Keis K, Lindquist S E and Hagfeldt A 2001 *J. Phys. Chem.* B **105** 3350

[18] Liu B and Zeng H C 2003 *J. Am. Chem. Soc.* **125** 4430

[19] Qiu Z, Wong K S, Wu M, Lin W and Xu H 2004 *Appl. Phys. Lett.* **84** 2739

[20] Sun X M, Chen X, Deng Z X and Li Y D 2002 *Mater. Chem. Phys.* **78** 99

[21] Pauling L 1954 *General Chemistry* 2nd edn (San Francisco, CA: Freeman)

[22] Xu C X and Sun X W 2003 *Japan. J. Appl. Phys.* **42** 4949

List of Figures

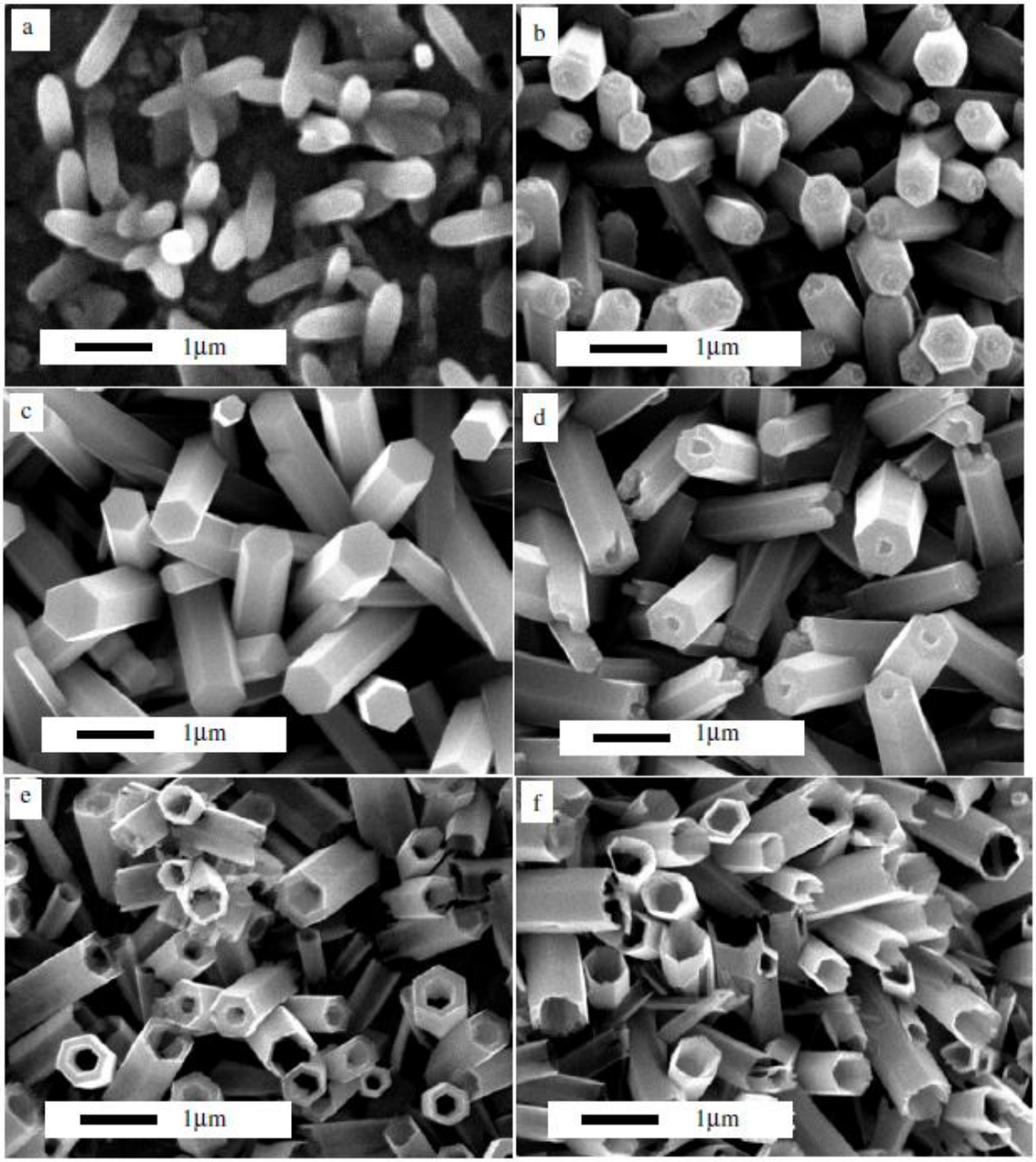

Figure 1

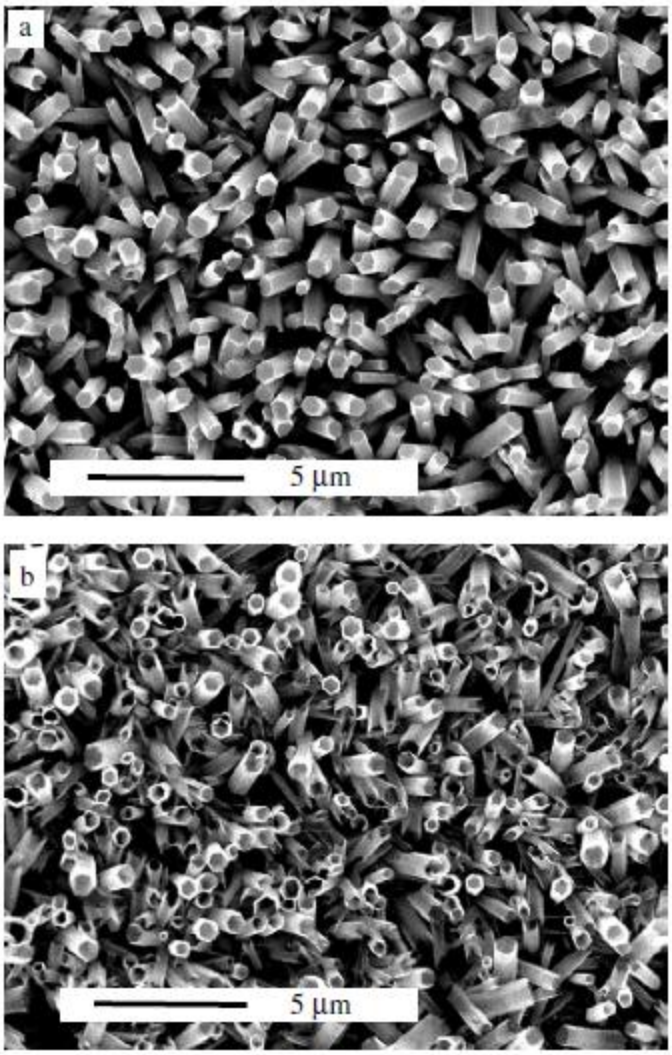

Figure 2

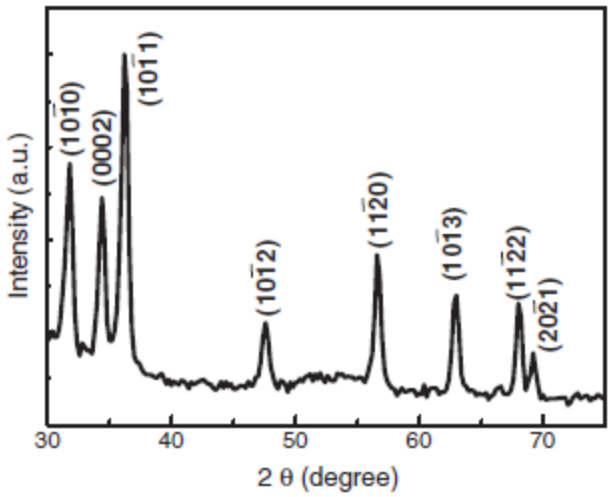
Intensity (a.u.)
(10$\bar{1}$0)
(0002)
(10$\bar{1}$1)
(10$\bar{1}$2)
(11$\bar{2}$0)
(10$\bar{1}$3)
(11$\bar{2}$2)
(20$\bar{2}$1)
30
40
50
60
70
2 θ (degree)

Figure 3

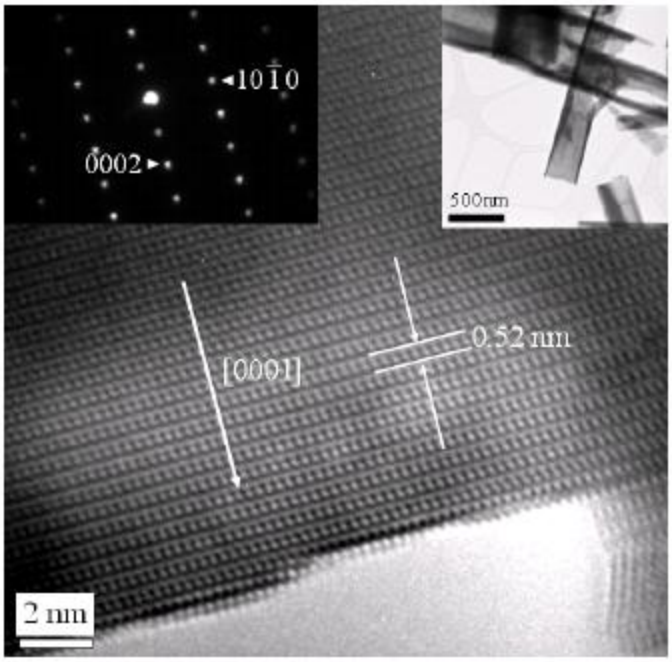

Figure 4

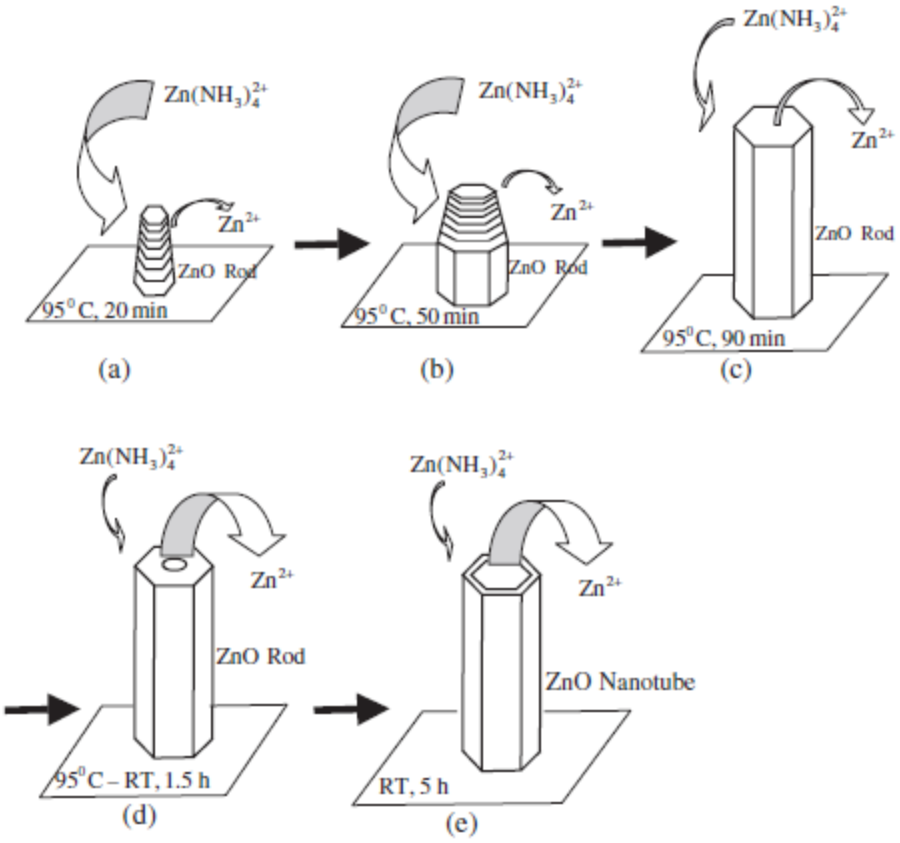
$Zn(NH_3)_4^{2+}$
Zn^{2+}
ZnO Rod
95°C, 20 min
(a)
95°C, 50 min
(b)
95°C, 90 min
(c)
ZnO Nanotube
95°C – RT, 1.5 h
(d)
RT, 5 h
(e)

Figure 5

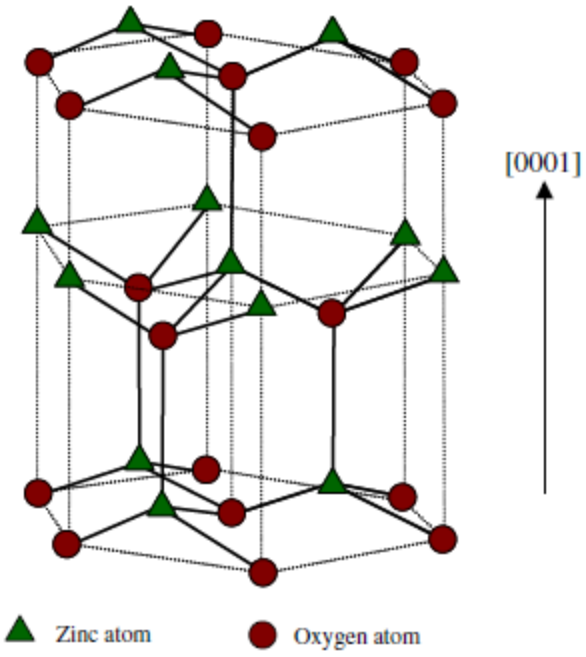

Figure 6